

Quantum dot nucleation in strained-layer epitaxy: minimum-energy pathway in the stress-driven 2D-3D transformation

José Emilio Prieto*

*Centro de Microanálisis de Materiales and Instituto Universitario “Nicolás Cabrera”,
Universidad Autónoma de Madrid, E-28049 Madrid, Spain*

Ivan Markov†

Institute of Physical Chemistry, Bulgarian Academy of Sciences, 1113 Sofia, Bulgaria

(Dated: August 26, 2018)

The transformation of monolayer islands into bilayer islands as a first step of the overall two-dimensional to three-dimensional (2D-3D) transformation in the coherent Stranski-Krastanov mode of growth is studied for the cases of expanded and compressed overlayers. Compressed overlayers display a nucleation-like behavior: the energy accompanying the transformation process displays a maximum at some critical number of atoms, which is small for large enough values of the misfit, and then decreases gradually down to the completion of the transformation, non-monotonically due to the atomistics of the process. On the contrary, the energy change in expanded overlayers increases up to close to the completion of the transformation and then abruptly collapses with the disappearance of the monoatomic steps to produce low-energy facets. This kind of transformation takes place only in materials with strong interatomic bonding. Softer materials under tensile stress are expected to grow predominantly with a planar morphology until misfit dislocations are introduced, or to transform into 3D islands by a different mechanism. It is concluded that the coherent Stranski-Krastanov growth in expanded overlayers is much less probable than in compressed ones for kinetic reasons.

PACS numbers: 68.35.Md, 68.35.Np, 68.65.Hb, 68.43.Hn

I. INTRODUCTION

Understanding the mechanism of transition from a planar two-dimensional (2D) thin film to a three-dimensional (3D) island morphology in the heteroepitaxy of highly mismatched materials is of crucial importance for the growth of self-assembled quantum dots in nanoscale technology. In the *coherent* Stranski-Krastanov (SK) mode of growth, dislocation-free 3D islands develop on top of a 2D wetting layer in order to relieve the misfit strain at the expense of an increase in surface energy.¹ This mechanism of strain relaxation is established in a multitude of systems of technological importance for the manufacturing of optoelectronic devices.² Despite the huge amount of studies devoted to the evolution of the cluster shape, many aspects, in particular the very beginning of the 2D-3D transition, still remain unclear.

The first theoretical concept for the transition from a 2D layer to faceted 3D islands included a nucleation mechanism as a result of the interplay between the surface energy and the relaxation of the strain energy relative to the values of the wetting layer.³ Irreversible 3D growth was predicted to begin above a critical volume, overcoming an energetic barrier whose height is inversely proportional to the forth power of the lattice misfit.

Mo *et al.* observed Ge islands representing elongated pyramids (“huts”) bounded by {105} facets inclined by 11.3° to the substrate.⁴ These clusters were thought to be a step in the pathway to the formation of larger islands with steeper side walls (“domes” or “barns”).⁵ Chen *et al.* studied the earliest stages of Ge islanding and found

that Ge islands smaller than the hut clusters do not involve discrete {105} facets.⁶ This result was later confirmed by Vailionis *et al.* who observed the formation of 3-4 monolayers-high “prepyramids” with rounded bases which existed over a narrow range of Ge coverages in the beginning of the 2D-3D transformation.⁷ Sutter and Lagally⁸ assumed that faceted, low-misfit alloy 3D islands can result from morphological instabilities (ripples) that are inherent to strained films,^{9,10,11} thus suggesting that 3D islands can be formed without the necessity to overcome a nucleation barrier. Similar views were simultaneously expressed by Tromp *et al.*¹² Tersoff *et al.* developed further this idea suggesting that the transition from the initial smooth “prepyramids” to faceted pyramids can be explained by assuming that the polar diagram of SiGe alloy islands allows the existence of all orientations vicinal to (001) with the first facet being {105}.¹³

In order to explain the experimental observation that SiGe alloy films roughen only under compressive stresses larger than a critical value of 1.4 %, Xie *et al.* assumed that the smallest 3D islands have stepped rather than faceted side surfaces.¹⁴ They noted that the steps on the SiGe(001) vicinals are under tensile stress and their energy of formation is lowered by the compressive misfit but increased by the tensile strain [see also the discussion in Refs. (15) and (16)]. As a result, the step formation and in turn the roughening are favored by the compressive misfit. It is worth noting that a barrierless evolution of stepped islands was predicted by Sutter and Lagally under the assumption that the slope of the side walls of the stepped islands increases continuously from zero to

11.3°.⁸

Priester and Lannoo suggested that 2D islands of monolayer height appear as precursors of the 3D islands.¹⁷ In addition, it was established that the minimum-energy pathway of the 2D-3D transition has to consist of a series of intermediate states with thicknesses increasing in monolayer steps and which are stable in separate intervals of volume. The first step in this transformation should be the rearrangement of monolayer into bilayer islands.^{18,19} Khor and Das Sarma found by Monte Carlo simulations that during the rearrangement, the material for the bilayer island comes almost completely from the original monolayer island, the bulk of the material for the three-layer island comes from the original two-layer island, etc.²⁰

Moison *et al.* reported that the coverage suddenly decreases from about 1.75 ML to 1.2 ML when 3D InAs islands begin to form on GaAs.²¹ The same phenomenon has been observed by Shklyav *et al.* in the case of Ge/Si(111).²² These observations suggest a process of rearrangement as mentioned above. Voigtländer and Zinner noted that 3D Ge islands have been observed in the same locations on the Si(111) surface where 2D islands locally exceeded the critical thickness of the wetting layer of two bilayers.²³ One-monolayer thick InAs islands were suggested to act as precursors for formation of thicker structures on GaAs.²⁴ The simultaneous presence of stable one, two, three or four monolayers-thick islands has been observed in heteroepitaxy of InAs on InP and GaAs.^{25,26,27}

In this paper we studied the earliest stages of growth of thin films in the coherent (dislocation-free) Stranski-Krastanov mode. We considered the instability of the planar growth against clustering by focussing on the conservative (i.e., without considering further deposition) mono- to bilayer transformation as a first step of the overall 2D-3D transition, or the beginning of the formation of the “prepyramids” mentioned above. We found that this transformation is a true nucleation process in compressed overlayers, in the sense that a critical nucleus of the second layer is initially formed and then grows further up to the complete mono-bilayer transformation. The energy associated with the transformation thus reaches a maximum and then starts a decreasing trend.²⁸ This is not the case in expanded overlayers, where the energy tends to increase up to very close to the completion of the transformation and then steeply decreases at the very end. The main result of this study is that coherent Stranski-Krastanov growth in expanded overlayers is much less probable than in compressed ones.

II. MODEL

We consider an atomistic model in $2 + 1$ dimensions. The 3D crystallites have *fcc* structure and (100) surface orientation, thus possessing the shape of truncated square pyramids. We found that monolayer-high elongated

islands always have higher energy than square islands with the same number of atoms, as expected from the symmetry of the lattice and the isotropy of the interaction potentials (see below). The lattice misfit is the same in both orthogonal directions. We consider interactions only in the first coordination sphere; inclusion of further coordination spheres does not alter qualitatively the results.

The choice of crystal lattice and interaction potential is more appropriate for the heteroepitaxy of (close-packed) metals on metals rather than for that of semiconductor materials. As a consequence, properties that depend crucially on the strong directional bonding characteristic of semiconductors cannot be addressed by our model. Some examples are: the dependence of the shape of GeSi/Si dots on volume^{4,5,6} as discussed above; the observation of lens-shaped^{29,30} and pyramidal³¹ dots and even of coexistence of both types³² in InAs/GaAs, the other well-studied system (for a recent review see Ref. 33) or the cases where the accommodation of the lattice misfit of a given material on different crystallographic faces of the same substrate takes place by other mechanisms (also found for InAs/GaAs),³⁴ where additional aspects as the presence of different surface reconstructions affect the thermodynamical balance of surface energies as well as the diffusion kinetics and, as a consequence, the nucleation behaviour and the growth mode. As our aim is to study the “reversible” minimum-energy pathway of the transition from metastable states to the ground state of a given system, the exact particularities of the model are not likely to play a crucial role and we expect the same qualitative behavior for any crystal lattice, crystal shape and interatomic potential.

We have performed atomistic calculations making use of a simple minimization procedure. The atoms interact through a pair potential whose anharmonicity can be varied by adjusting two constants μ and ν ($\mu > \nu$) that govern separately the repulsive and the attractive branches, respectively,^{35,36}

$$V(r) = V_o \left[\frac{\nu}{\mu - \nu} e^{-\mu(r-b)} - \frac{\mu}{\mu - \nu} e^{-\nu(r-b)} \right], \quad (1)$$

where b is the equilibrium atom separation. For $\mu = 2\nu$ the potential (1) turns into the familiar Morse form.

A static relaxation of the system is performed by allowing each atom to displace in the direction of the force, i.e., the gradient of the energy with respect to the atomic coordinates, in an iterative procedure until all the forces fall below some negligible cutoff value. As we were only interested in the 2D-3D transformation of isolated islands, the calculations were performed under the assumption that the substrate (the wetting layer) is rigid; the atoms there are separated by a distance a . The lattice misfit is thus given by $\varepsilon = (b - a)/a$.

For the study of the mechanism of mono-bilayer transformation, we assume the following imaginary model process:³⁷ atoms detach from the edges of monolayer islands, which are larger than the critical size for the mono-

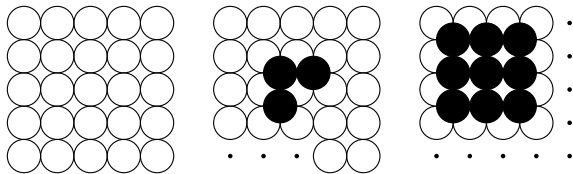


FIG. 1: Schematic process for the evaluation of the activation energy of the monolayer-bilayer transformation. The initial state is a square monolayer island. The intermediate state is a monolayer island short of some number of atoms which are detached from the edges and placed in the second level. The final state is a truncated bilayer pyramid.

to bilayer transformation N_{12} and thus unstable against bilayer islands, diffuse on top of them, aggregate and give rise to second-layer nuclei. These grow at the expense of the atoms detached from the edges of the lower islands. The process continues up to the moment when the upper island completely covers the lower-level island. To simulate this process, we assume an initial square monolayer island, detach atoms one by one from its edges and locate them on top and at the center of the ML island, building there structures as compact as possible (Fig. 1). The energy change associated with the process of transformation at a particular stage is given by the difference between the energy of the incomplete bilayer island and that of the initial monolayer island. This is in fact a conservative version of the mechanism observed by Khor and Das Sarma in 1+1 dimensions.²⁰

III. RESULTS

A. Stability of Monolayer Islands

In our previous work in (1+1)D models, it was established that monolayer-high islands are stable against bilayer islands up to some critical volume or number of atoms N_{12} ; in turn, bilayer islands are stable against trilayer islands up to another critical number $N_{23} > N_{12}$; etc.^{18,19} The mono-bilayer transformation was considered as the first step of the overall 2D-3D transformation and a critical misfit was determined from the misfit dependence of N_{12} . The latter was found to increase with decreasing misfit diverging at a critical value ε_{12} . Above the critical misfit, the coherent Stranski-Krastanov mode is favored against the layer-by-layer growth followed by introduction of misfit dislocations. The opposite is true below the critical value. Whereas this critical behavior is clearly pronounced with compressive strain, it is much smoother in expanded overlayers. It is worth noting that the existence of critical misfit was observed in a series of heteroepitaxial systems.^{14,30,38,39}

In the present work, using more realistic (2+1)D models, we found a larger difference in the behavior of expanded and compressed overlayers. Figure 2 shows that the total energies of mono- and bilayer islands under ten-

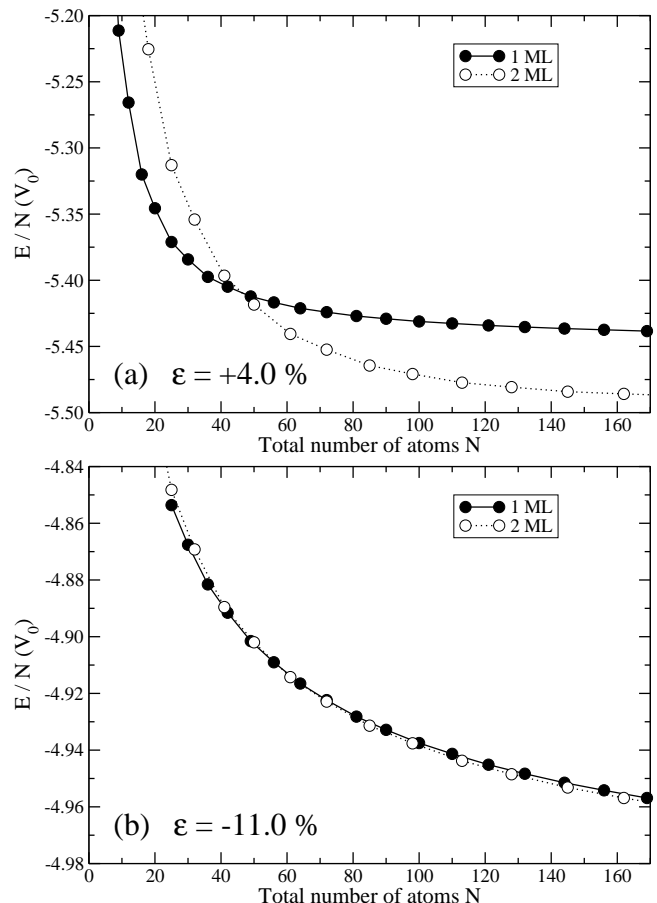


FIG. 2: Total energy per atom of mono- and bilayer islands at (a) positive (+4.0 %) and (b) negative (-11.0 %) values of the misfit as a function of the total number of atoms. The potential is of the form given by eq. (1) with $\mu = 16$ and $\nu = 14$.

sile stress containing the same total number of atoms are very close to each other compared with the corresponding behavior in compressed overlayers. As will be shown below this leads to the conclusion that even for $N \gg N_{12}$, determined as the crossing point of the curves corresponding to monolayer and bilayer islands in Fig. 2, the probability of the 2D-3D transformation remains nearly equal to the probability of the reverse 3D-2D transformation.

It turns out that the misfit dependence of N_{12} is very sensitive to the value of the force constant $\gamma = \mu\nu V_0$ of the interatomic bonds, particularly in expanded overlayers (Fig. 3). Decreasing μ and ν (V_0 is assumed equal to unity) in such a way that the ratio μ/ν is kept constant (in this case equal to 8/7), shifts the intersection points N_{12} to larger absolute values of the misfit. As a result, a critical size N_{12} in compressed overlayers exists practically for all values of γ whereas in overlayers under tensile stress, N_{12} shifts to so large values of the misfit that they effectively disappear below some critical value of γ .

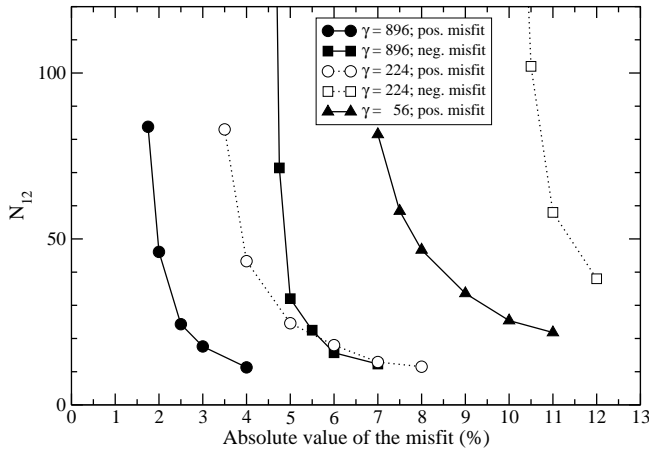


FIG. 3: Critical island size N_{12} (number of atoms) as a function of the lattice mismatch at different values of the force constant $\gamma = \mu\nu V_0$. Potentials of the form given by eq. (1) were used, with $\mu/\nu = 8/7$ (V_0 is taken equal to unity). As seen, coherent 3D islanding is favored in expanded overlayers only in “stiffer” materials.

It was established that in the case of a force constant of an intermediate value ($\mu = 2\nu = 12$), N_{12} disappears (the monolayer islands are always stable against bilayer islands), but $N_{13}, N_{14}, N_{23}...$ still exist. This points to a novel mechanism of 2D-3D transformation which differs from the consecutive formation of bilayer, trilayer, etc. islands, each from the previous one. The new mechanism obviously consists of the formation and 2D growth of bilayer islands on top of the monolayer island, thus transforming the initial monolayer island directly into a trilayer island. At even smaller values of γ , the critical values N_{13}, N_{14} etc. consecutively disappear, suggesting a generalized mechanism of 2D-3D transformation in which the monolayer islands transform into thicker islands. This multilayer 2D mechanism will be a subject of a separate study. In this paper we focus on the layer-by-layer 2D-3D transformation.

We considered also the stability of monolayer islands against bilayer islands with a different slope of the side walls. It was found that N_{12} is smaller if the slope of the side walls is the steepest one (60°) for this lattice in comparison with flatter islands (Fig. 4). This is due to the fact that in crystals with steeper side walls, the strain relaxation is more efficient than in flatter islands. This is in contradiction with the experiments in semiconductor growth in which islands with side walls of a smaller slope than that of the first facet are initially observed.^{6,7,14} In any case this means that we can exclude the flatter islands from our consideration.

We conclude that for some reasonable degree of anharmonicity (e.g. $\mu = 2\nu$ in our model), monolayer islands become unstable against bilayer islands thus making possible the 2D-3D transformation by the layer-by-layer mechanism only at strong enough interatomic bonding. Soft materials are expected to grow either with a pla-

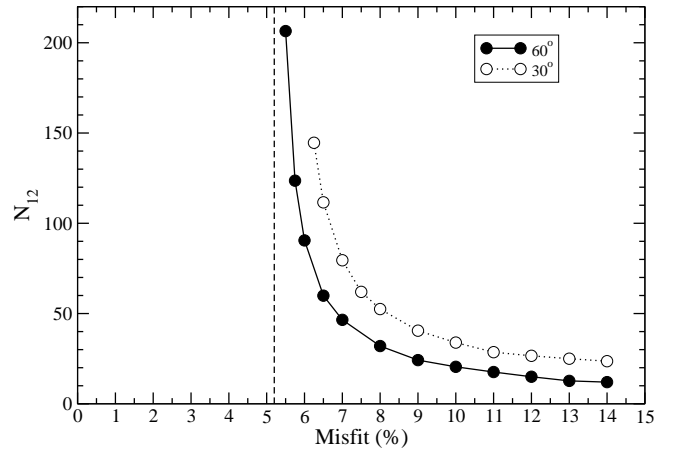


FIG. 4: Misfit dependence of the critical sizes N_{12} of mono- and bilayer islands with different shapes, given by different angles of the side walls: 60° and 30° ($\mu = 2\nu = 12$). The critical misfit ε_{12} is shown by the vertical dashed line.

nar morphology until misfit dislocations are introduced or to transform into 3D islands by a different, multilayer 2D mechanism.

B. Mechanism of 2D-3D transformation

Figure 5 shows typical transformation curves of the energy change as a function of the number of atoms in the upper island for (a) positive and (b) negative misfits. It is immediately seen that in a compressed overlayer, the transformation curve for ΔG has the typical shape of a nucleus formation curve: it displays a maximum ΔG_{max} for a cluster consisting of a small number of atoms n_{max} and then decreases beyond this size up to the completion of the transformation. The atomistics of the transfer process (i.e. the completion of rows in the upper level and their depletion in the lower one) is responsible for the jumps (the non-monotonic behaviour) in the curve.

In the case of expanded overlayers, the energy change increases up to a large number of atoms (again non-monotonically due to the atomistics) and then abruptly decreases at the end of the transformation. No true maximum is displayed. The energy change becomes negative only after the transfer of the last several atoms. Comparing the largest value of the energy with the energy at the transformation completion leads to the conclusion that the probabilities of the direct and reverse transformations are nearly equal.

Figure 6 depicts the evolution of the height of the barrier ΔG_{max} as a function of misfit (in expanded overlayers, this is the highest value reached before the collapse of the energy). The figures at each point show the number of atoms in the cluster at the maximum of the transformation curve. As seen, in the case of compressed overlayers, ΔG_{max} decreases steeply with increasing misfit in a way similar to the decrease of the work required

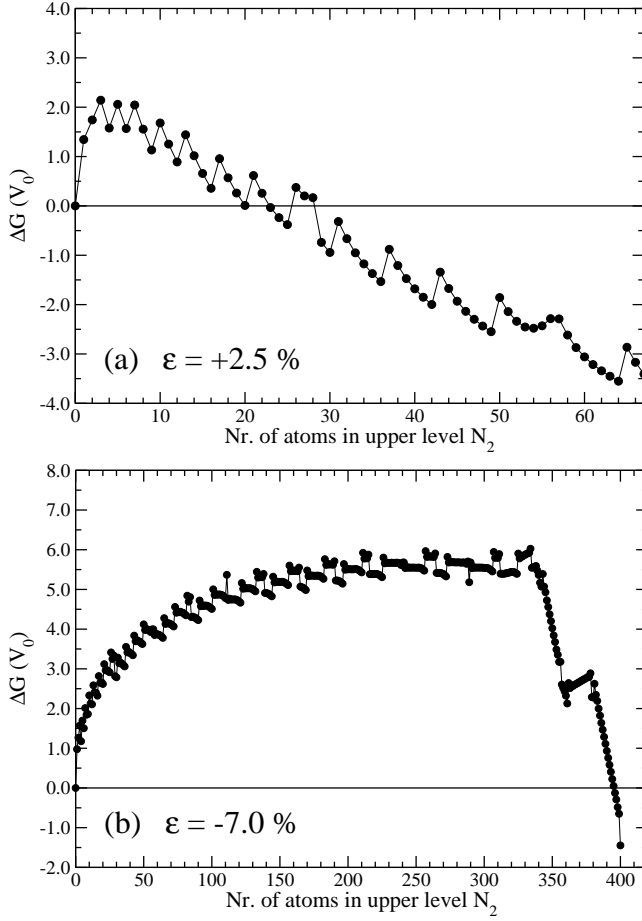


FIG. 5: Transformation curves representing the energy change in units of the bond energy V_0 as a function of the number of atoms in the upper level for (a) positive (+2.5 %) and (b) negative (-7.0 %) values of the misfit. The number of atoms in the initial monolayer island ($N_0 = 841 = 29 \times 29$) is chosen in such a way that the resulting truncated bilayer pyramid is complete ($21 \times 21 = 441$ atoms in the lower and $20 \times 20 = 400$ atoms in the upper level); $\mu = 2\nu = 36$.

for nucleus formation with increasing supersaturation in the classical theory of nucleation.²⁸ Assuming a dependence of the kind $\Delta G = K\varepsilon^{-n}$ where K is a constant proportional to the Young modulus (or the force constant γ) and ε is the lattice misfit, we found $n = 4.29$ for $\mu = 12, \nu = 6$, and $n = 4.75$ for $\mu = 36, \nu = 18$. It is worth noting that assuming 3D nucleation on top of the wetting layer, Grabow and Gilmer predicted a value $n = 4$ for small misfits (large nuclei) assuming that ΔG_{max} is inversely proportional to the square of the supersaturation, which in turn is proportional to the square of the lattice misfit.⁴⁰ Note that the same exponent of four was obtained also by Tersoff and LeGoues.³ Obviously, in our case the exponent n is a complicated function of the force constant in the interatomic bonds but the value of the exponent is of the same order.

The misfit behavior of the critical nucleus size n_{max} is also similar to that found in the theory of nucleation.

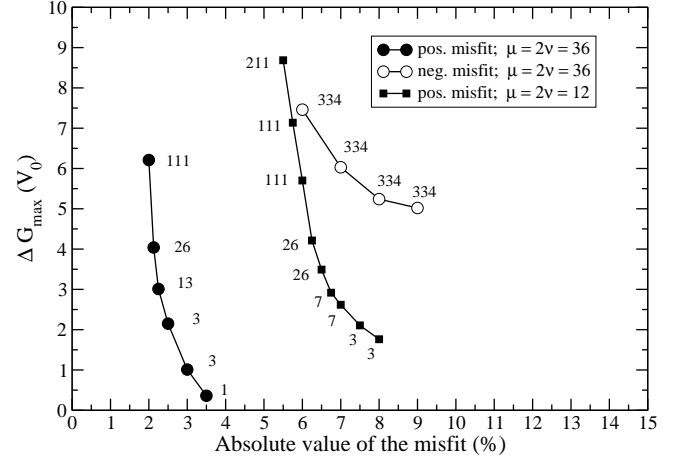


FIG. 6: Height of the energetic barriers in units of V_0 as a function of the absolute value of the lattice misfit. The figures at each point show the number of atoms in the critical nucleus n_{max} . The initial island size was $29 \times 29 = 841$ atoms. The round symbols were calculated for $\mu = 2\nu = 36$, the squares for $\mu = 2\nu = 12$.

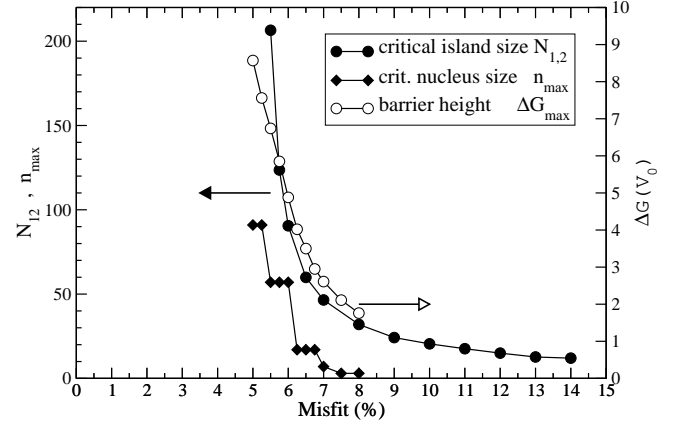


FIG. 7: Misfit dependence of the critical island size N_{12} , the critical nucleus size n_{max} , (both expressed in number of atoms), and the nucleation barrier height ΔG_{max} (in units of V_0) for compressed overlayers and $\mu = 2\nu = 12$. The last two magnitudes were computed for islands of an initial size of $20 \times 20 = 400$ atoms.

The nucleus size decreases with increasing misfit, reaching eventually only one atom just as the nucleus size on the supersaturation in nucleation theory.²⁸ It is interesting to note that the critical nuclei contain always a number of atoms which *exceeds* by one atom the size of a compact cluster, and is *not* one atom short of being a compact cluster, as might be expected from too-simplistic energetic considerations on the basis of bond-counting arguments. The reason is that the highest departure from compactness giving the maximum of the ΔG curve is achieved when the additional atom creates two kink positions for the attachment of the next row of atoms.

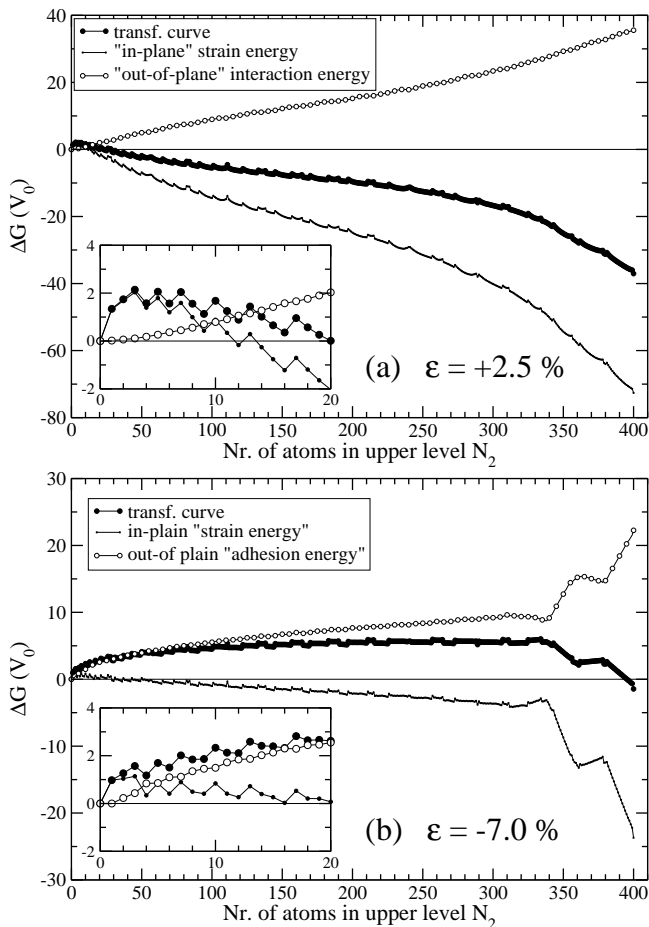


FIG. 8: Variation of the in-plane strain energy and out-of-plane interaction energies during the mono-bilayer transformation process in (a) compressed ($\epsilon = +2.5\%$) and (b) expanded ($\epsilon = -7.0\%$) overlayers with $\mu = 2\nu = 36$. The initial sizes of the islands were $29 \times 29 = 841$ atoms. The inserts show the curves at the beginning of the transformation with enlarged scales.

On the contrary, in expanded overlayers, the number of atoms at which the transformation curve reaches its highest value does not depend on the misfit (Fig. 6), demonstrating the non-nucleation behavior of the process. This number is roughly equal to the number of atoms which completes the upper level minus the number of atoms required to build the last four edge rows of the upper level in order to produce four facets. A special feature of the above results is that the barriers for expanded overlayers are in general larger than those for compressed overlayers. Having in mind that the typical time needed for the transformation to occur is inversely proportional to $\exp(-\Delta G_{max}/kT)$, we have to expect much longer times for the occurrence of the 2D-3D transformation in expanded overlayers as compared with compressed ones particularly at larger values of the misfit. Thus limitations of kinetic origin (astronomically long times for second layer nucleation) are expected in

expanded overlayers and at small misfits in compressed overlayers.

Figure 7 compares the misfit dependences of the critical island size N_{12} , the critical 2nd-layer nucleus size n_{max} and the height of the nucleation barrier ΔG_{max} for compressed overlayers. The three curves display a similar behavior increasing steeply with decreasing misfit, with N_{12} showing a critical behavior at the critical misfit ϵ_{12} . As will be discussed below, the 2D-3D transformation will be inhibited for kinetic reasons at values of the misfit not sufficiently larger than ϵ_{12} .

IV. DISCUSSION

In compressed overlayers the atoms interact with their in-plane neighbours through the steeper repulsive branch of the interatomic potential. This means that compressed overlayers are effectively “stiffer” than expanded overlayers. Then compressed pseudomorphic overlayers will contain a larger amount of elastic energy than expanded pseudomorphic ones of the same thickness and bonding strength. Another consequence is that the accumulation of strain energy with thickness in compressed overlayers will be steeper than in expanded overlayers. Or, the strain energy of a bilayer will differ considerably from that of a monolayer from both sides of the critical size N_{12} compared with expanded islands as seen in Fig. 2. This is the reason why expanded overlayers require greater force constants in order for the monolayer islands to become unstable against bilayer islands. This is also the reason why the critical sizes N_{12} are larger in expanded than in compressed overlayers of the same force constant as seen in Fig. 3.

Figure 5 illustrates the central result of our study. It shows the energy of transformation of compressed and expanded monolayer islands. In compressed overlayers the overall fall of the energy begins when a small cluster (three atoms in this particular case) is formed in the second level. This is a typical phase transition of first order - nucleation followed by irreversible growth.³⁷ In expanded overlayers the energy increases up to nearly the end of the transformation and then abruptly collapses. This collapse of the energy is connected with the transfer of the remaining last edge rows of atoms which leads to the coalescence of the lower and upper steps to produce four side facets. In the particular transfer process considered in the calculation, there are two regions, one before the beginning of the collapse, the second between the two sub-collapses, where the total energy rises slightly; this is due to the energetic cost of repulsion between steps that are very close, separated only by a single atomic row. The reason for this “non-nucleation” behavior is the effectively weaker expanded bonds which results in relatively close energies of the monolayer and bilayer islands. With increasing size of the second level cluster, the misfit strain is not as effectively relaxed as in the case of compressed islands and the collapse of the energy

is due to the replacements of isolated repulsing steps by low-energy facets.

The different transformation behavior can be understood on the basis of the above considerations accounting in addition for the finite size of the islands. During the transformation of the monolayer islands we should expect a relaxation of the in-plane strain, which is the driving force for the transformation and an increase of the total energy of interaction between the lower level of the island and the substrate and between both levels of the island.^{18,19}

The physics behind the process of mono-bilayer transformation is the same as behind the formation of 3D islands on the wetting layer.^{3,41} Formation and growth of new steps and relaxation of the strain stored in the monolayer island compete in the process. In addition, the steps in the first and second levels repel each other and the associated repulsion energy increases towards the completion of the transformation to disappear when the steps coalesce to give rise to microfacets.

Epitaxial strain is relaxed at the islands edges.⁴² Edge atoms are displaced from the bottoms of their respective potential troughs giving rise to relaxation of the bonds parallel to the surface (in-plane stress relaxation). The displaced atoms loose contact with the substrate atoms, which leads to an increase of the out-of-plane energy of interaction with the underlying substrate.^{43,44} During the transformation, new edges on top of the initial monolayer island are formed and the total length of the edges increases as $\Delta L(N_2) = 4(\sqrt{N_0 - N_2} + \sqrt{N_2} - \sqrt{N_0})$ where N_0 and N_2 are the number of atoms in the initial monolayer island and the current number of transferred atoms in the second level, respectively. Note that the energy of repulsion between the edges bounding the lower and upper islands is implicitly accounted for by both the in-plane and out-of-plane energies. Then a larger number of atoms are displaced from the bottom of their respective potential troughs during the transformation process and the total in-plane strain-relaxation energy decreases. Simultaneously, the out-of-plane interaction energy increases. Owing to the weaker attractive forces in expanded overlayers, only a small number of bonds close to the edges are relaxed.¹⁹ Most of the bonds at the center of the islands are strained to fit the underlying wetting layer. As a result, the average relaxation in expanded islands is smaller than in compressed islands, where even bonds at the center of medium-sized islands are partly relaxed. In compressed overlayers, the decrease of the in-plane strain energy rapidly overcompensates the increase of the out-of-plane interaction energy which results in a nucleation-like transformation curve (Fig. 8). In expanded overlayers, the absolute value of the total in-plane strain energy is smaller than the out-of-plane interaction energy with the exception of the final stage when the monolayer-high steps disappear to produce facets of small surface energy.

The typical time required for the appearance of a

second-layer nucleus is inversely proportional to the nucleation frequency $\omega = S_{12}K \exp(-\Delta G_{max}/kT)$, where $S_{12} = a^2 N_{12}$ is the area of the critical monolayer island and K is the pre-exponential of the nucleation rate. As seen in Fig. 6, in the case of $\mu = 2\nu = 12$, the barrier height increases approximately 5 times in an interval of ε of 2.5 % whereas the number of atoms in the critical nucleus n_{max} increases nearly 70 times. For a greater force constant ($\mu = 2\nu = 36$), the increase of both ΔG_{max} and n_{max} is even larger: 20 and 110 times, respectively, in a smaller misfit interval of about 1.5 %. The energy to break a first-neighbor bond, V_0 , for most semiconductor materials is of the order of 2 to 2.5 eV (the enthalpy of evaporation is of the order of 4 to 5 eV). Assuming N_{12} is of the order of 100 - 120 atoms we could expect a mono-bilayer transformation to take place at misfits for which $\Delta G_{max}/kT < 15 - 20$ ($n_{max} \leq 3$). The reason is that the pre-exponential K in 2D nucleation rate from vapor is usually of the order of $10^{20} \text{ cm}^{-2} \text{ s}^{-1}$.²⁸ Otherwise, due to the exponential dependence, times of the order of centuries would be required for second-layer nucleation.⁴⁵ Thus, although in compressed overlayers second-layer nucleation can be expected for thermodynamic reasons at misfits above ε_{12} , a real 2D-3D transition can only take place at even larger misfits or higher temperatures for kinetic reasons. As the height of the transformation barriers in expanded overlayers is always greater than several times V_0 , the mono-bilayer transformation should be strongly inhibited for kinetic reasons.

We conclude that the case of a layer-by-layer mechanism for the 2D-3D transformation is expected only in compressed overlayers at misfits sufficiently larger than ε_{12} . The reason is that the mechanism of the mono-bilayer transformation is nucleation-like due to the interplay of relaxation of the in-plane strain, which is proportional to the total edge length and the increase of the total edge energy and repulsion between the edges. The transformation curve in expanded overlayers shows a “non-nucleation” behavior characterized by an overall increase of the energy up to the stage when the single steps coalesce to produce low-energy facets. The latter is accompanied by a collapse of the energy. The maximum energy is large and 2D-3D transformation of expanded overlayers is not expected for kinetic reasons even for materials with strong interatomic bonds. Softer materials are expected to grow with a planar morphology until misfit dislocations are introduced, or to transform into 3D islands by a different mechanism.

Acknowledgments

J.E.P. gratefully acknowledges financiación by the programme “Ramón y Cajal” of the Spanish Ministerio de Educación y Ciencia.

-
- * Electronic address: joseemilio.prieto@uam.es
† Electronic address: imarkov@ipchp.ipc.bas.bg
- ¹ D.J. Eaglesham and M. Cerullo, Phys. Rev. Lett. **64**, 1943 (1990).
 - ² B.A. Joyce, P.C. Kelires, A.G. Naumovets, and D.D. Vvedensky, eds. *Quantum Dots: Fundamentals, Applications and Frontiers*, NATO Science Series, II. Mathematics, Physics and Chemistry - Vol. 190, (Springer, 2005).
 - ³ J. Tersoff and F.K. LeGoues, Phys. Rev. Lett. **72**, 3570 (1994).
 - ⁴ Y.-W. Mo, D.E. Savage, B.S. Swartzentruber, and M.G. Lagally, Phys. Rev. Lett. **65**, 1020 (1990).
 - ⁵ E. Sutter, P. Sutter, and J.E. Bernard, Appl. Phys. Lett. **84**, 2262 (2004).
 - ⁶ K.M. Chen, D.E. Jesson, S.J. Pennycook, T. Thundat, and R.J. Warmack, Phys. Rev. B **56**, R1700 (1997).
 - ⁷ A. Vailionis, B. Cho, G. Glass, P. Desjardins, D.G. Cahill, and J.E. Greene, Phys. Rev. Lett. **85**, 3672 (2000).
 - ⁸ P. Sutter and M.G. Lagally, Phys. Rev. Lett. **84**, 4637 (2000).
 - ⁹ R.J. Asaro and W.A. Tiller, Metal. Trans. **3**, 1789 (1972).
 - ¹⁰ M. Ya. Grinfeld, Sov. Phys. Dokl. **31**, 831 (1986).
 - ¹¹ D. J. Srolovitz, Acta Metall. **37**, 621 (1989).
 - ¹² R.M. Tromp, F.M. Ross, and M.C. Reuter, Phys. Rev. Lett. **84**, 4641 (2000).
 - ¹³ J. Tersoff, B.J. Spencer, A. Rastelli, and H. von Känel, Phys. Rev. Lett. **89**, 196104 (2002).
 - ¹⁴ Y.H. Xie, G.H. Gilmer, C. Roland, P.J. Silverman, S.K. Buratto, J.Y. Cheng, E.A. Fitzgerald, A.R. Kortan, S. Schuppler, M.A. Marcus, and P.H. Citrin, Phys. Rev. Lett. **73**, 3006 (1994).
 - ¹⁵ J. Tersoff, Phys. Rev. Lett. **74**, 4962 (1995).
 - ¹⁶ Y.H. Xie *et al.* Phys. Rev. Lett. **74**, 4963 (1995).
 - ¹⁷ C. Priester and M. Lannoo, Phys. Rev. Lett. **75**, 93 (1995).
 - ¹⁸ E. Korutcheva, A.M. Turiel and I. Markov, Phys. Rev. B **61**, 16890 (2000).
 - ¹⁹ J.E. Prieto and I. Markov, Phys. Rev. B **66**, 073408 (2002).
 - ²⁰ K.E. Khor and S. Das Sarma, Phys. Rev. B **62**, 16657 (2000).
 - ²¹ J.M. Moison, F. Houzay, F. Barthe, L. Leprince, E. André, and O. Vatel, Appl. Phys. Lett. **64**, 196 (1994).
 - ²² A. Shklyae, M. Shibata, and M. Ichikawa, Surf. Sci. **416**, 192 (1998).
 - ²³ B. Voigtländer and A. Zinner, Appl. Phys. Lett. **63**, 3055 (1993).
 - ²⁴ A. Polimeni, A. Patane, M. Capizzi, F. Martelli, L. Nasi, and G. Salviati, Phys. Rev. B **53**, R4213 (1996).
 - ²⁵ A. Rudra, R. Houdré, J.F. Carlin, and M. Ilegems, J. Cryst. Growth **136**, 278 (1994).
 - ²⁶ R. Houdré, J.F. Carlin, A. Rudra, J. Ling, and M. Ilegems, Superlattices and Microstructures **13**, 67 (1993).
 - ²⁷ M. Colocci, F. Bogani, L. Carraresi, R. Mattolini, A. Bosacchi, S. Franchi, P. Frigeri, M. Rosa-Clot, and S. Taddei, Appl. Phys. Lett. **70**, 3140 (1997).
 - ²⁸ I. Markov, I. *Crystal Growth for Beginners*, 2nd edition, (World Scientific, 2003).
 - ²⁹ D.W. Pashley, J.H. Neave, and B.A. Joyce, Surf. Sci. **476**, 35 (2001).
 - ³⁰ T. Walthers, A.G. Cullis, D.J. Norris, and M. Hopkinson, Phys. Rev. Lett. **86**, 2381 (2001).
 - ³¹ K. Zhang, Ch. Heyn, W. Hansen, Th. Schmidt, and J. Falta, Appl. Phys. Lett. **76**, 2229 (2000).
 - ³² A.S. Bhatti, M. Grassi Alessi, M. Capizzi, P. Frigeri and S. Franchi, Phys. Rev. B **60**, 2592 (1999).
 - ³³ B.A. Joyce and D.D. Vvedensky, in *Atomistic Aspects of Epitaxial Growth*, ed. by M. Kotrla, N. I. Papanicolaou, D. D. Vvedensky and L. T. Wille, NATO Science Series II. Mathematics, Physics and Chemistry, Vol. 65, (Kluwer, 2002) p. 301.
 - ³⁴ B.A. Joyce, J.L. Sudijono, J.G. Belk, H. Yamaguchi, X.M. Zhang, H.T. Dobbs, A. Zangwill, D.D. Vvedensky, and T.S. Jones, Jpn. J. Appl. Phys. **36**, 4111 (1997).
 - ³⁵ I. Markov and A. Trayanov, J. Phys. C **21**, 2475 (1988).
 - ³⁶ I. Markov, Phys. Rev. B **48**, R14016 (1993).
 - ³⁷ S. Stoyanov and I. Markov, Surf. Sci. **116**, 313 (1982).
 - ³⁸ D. Leonard, M. Krishnamurthy, C.M. Reaves, S.P. Denbaars, and P.M. Petroff, Appl. Phys. Lett. **63**, 3203 (1993).
 - ³⁹ M. Pinczolis, G. Springholz and G. Bauer, Appl. Phys. Lett. **73**, 250 (1998).
 - ⁴⁰ M. Grabow and G. Gilmer, Surf. Sci. **194**, 333 (1988).
 - ⁴¹ C. Duport, C. Priester, and J. Villain, in *Morphological Organization in Epitaxial Growth and Removal*, Vol. 14 of *Directions in Condensed Matter Physics*, ed. by Z. Zhang and M. Lagally (World Scientific, Singapore, 1998).
 - ⁴² J. Villain, J. Crystal Growth **275**, e2307 (2005).
 - ⁴³ R. Niedermayer, Thin Films **1**, 25 (1968).
 - ⁴⁴ W.A. Jesser and J. H. van der Merwe, Surf. Sci. **31**, 229 (1972).
 - ⁴⁵ J.G. Dash, Phys. Rev. B **15**, 3136 (1977).